Evidence that Phosphate Release Is the Rate-Limiting Step on the Overall ATPase of Psoas Myofibrils Prevented from Shortening by Chemical Cross-Linking†

Corinne Lionne,*,‡ Bogdan Iorga,‡ Robin Candau,‡ Nicoletta Piroddi,§ Martin R. Webb,|| Alexandra Belus,§ Franck Travers,‡ and Tom Barman‡

INSERM U128, 1919 route de Mende, 34293 Montpellier Cedex 5, France, NIMR, Mill Hill, London NW7 1AA, United Kingdom, and Dipartimento di Scienze Fisiologiche, Università degli Studi di Firenze, Viale G. B. Morgagni, I-50134 Firenze, Italy

Received April 25, 2002; Revised Manuscript Received July 15, 2002

ABSTRACT: It has been suggested that the mechanical condition determines the rate-limiting step of the ATPase of the myosin heads in fibers: when fibers are isometrically contracting, the ADP release kinetics are rate-limiting, but as the strain is reduced and the fibers are allowed to shorten, the ADP release kinetics accelerate and P_i release becomes rate-limiting. We have put this idea to the test with myofibrils as a model because with these both mechanical and chemical kinetic measurements are possible. With relaxed or rapidly shortening myofibrils, P_i release is rate-limiting and (A)M·ADP·P_i states accumulate in the steady state [Lionne, C., et al. (1995) *FEBS Lett. 364*, 59]. We have now studied the kinetics of P_i release with chemically cross-linked myofibrils that, when adequately cross-linked, appear to be a good model for isometric contraction. By using a method that is specific for free P_i and rapid quench flow that measures the amount of (A)M·ADP·P_i states and free P_i, we show that (A)M·ADP·P_i states predominate which suggests that the overall ATPase is limited by P_i release kinetics. Therefore, under our experimental conditions with myofibrils prevented from shortening, the concentration of (A)M·ADP states is low, as with rapidly shortening and relaxed myofibrils. This result is difficult to reconcile with the sensitivity of force development in fibers and myofibrils to P_i which implies interaction of P_i with an (A)M·ADP state. We discuss two models for accommodating the mechanical and chemical kinetics with reference to the duty cycle in skeletal muscle.

Muscle contraction depends on the cyclic interaction of myosin heads (M) with actin (A), driven by the hydrolysis of ATP by the heads. This interaction is modulated by the nature of the ATPase intermediates. It is thought to be weak in (A)M·ATP and (A)M·ADP·P_i states and strong in (A)M and (A)M·ADP states (Scheme 1 and ref *1*).

Essentially, there are four events: ATP binding, rapid equilibrium (step 1) and a quasi irreversible isomerization (step 2); ATP cleavage (step 3); P_i release, isomerization (step 4) followed by escape (step 5); and ADP release, isomerization (step 6) followed by escape (step 7).

An important question concerns the transformation of the chemical energy provided by ATP hydrolysis by the myosin heads into mechanical energy, i.e., force and/or shortening. This mechanochemical coupling is thought to rely on conformational changes of the myosin heads that are connected with specific interactions of the different intermediates of the ATPase reaction pathway with the actin filament.

It is generally admitted that the product release steps are linked with the contractile process. Thus, P_i release is thought to be important in force generation (*2*, *3*) and ADP release in shortening (*4*, *5*), although the cleavage step may also be involved (*6*). Consequently, it has been proposed that the rate-limiting step on the ATPase reaction pathway is different during isometric contraction (high strain) and unloaded shortening (low strain). Geeves and Holmes (*7*) proposed that strain reduces *both* P_i and ADP release kinetics. From the P_i sensitivity of force development by muscle fibers, it has been suggested that a step involved in the ADP release is rate-limiting during isometric contraction (*8*−*10*). To summarize, it is proposed that when the mechanical condition is changed, there is a switch in the rate-limiting step: ADP release during isometric contraction and P_i release during unloaded shortening. This proposition can be put to the test by chemical kinetics, in particular, by the use of the free P_i probe of Brune et al. [a coumarin-labeled phosphate binding protein (*11*)]. Thus, with a rate-limiting ADP release, (A)M·ADP states accumulate and there is a transient burst of free P_i, whereas with a rate-limiting P_i release, the transient is due to bound P_i [in (A)M·ADP·P_i states]. In a preliminary publication, Ferenczi et al. (*12*) used the free P_i probe and proposed that with skinned cross-linked muscle fibers there is a change in the rate-limiting step when the strain is changed.

Our aim is to determine *directly* the rate-limiting step in the different states of contraction, on the same model, and under near-physiological conditions. We are using myofibrils as a model for muscle contraction because with these, both

† This work was supported by INSERM and the European Union (Contract HPRN-CT-2000-00091). B.I. and A.B. are recipients of EU fellowships.

* To whom correspondence should be addressed. E-mail: lionne@montp.inserm.fr. Telephone: +33-467-61-33-64. Fax: +33-467-52-36-81.

‡ INSERM U128.

§ Università degli Studi di Firenze.

|| NIMR.

10.1021/bi0260278 CCC: $22.00
Published on Web 10/11/2002

Scheme 1[a]

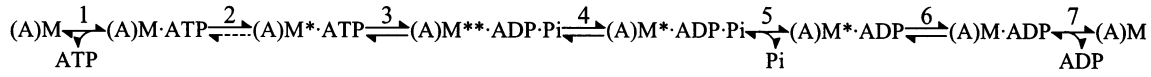

[a] One asterisk and two asterisks indicate different conformations of the myosin heads.

mechanical (*13*−*15*) and chemical kinetic (*16*−*18*) experiments are possible. Also, with such small biological systems, diffusion problems are avoided (*19*, *20*).

With relaxed or rapidly shortening myofibrils from both rabbit and frog fast skeletal muscles, we showed that the isomerization preceding P_i release (step 4 in Scheme 1) is rate-limiting so (A)M**·ADP·P_i states accumulate in the steady state (*21*, *22*). Here we studied the kinetics of P_i release with chemically cross-linked myofibrils that appear to be a good model for isometric contraction (*23*). By using the free P_i probe of Brune et al. (*11*) and rapid flow quench methods that measure the amounts of (A)M·ADP·P_i states and free P_i, we show that the ATPase of cross-linked myofibrils is apparently also limited by P_i release kinetics. Therefore, under our experimental conditions with myofibrils prevented from shortening, the (A)M·ADP·P_i states predominate and the concentration of (A)M·ADP states is low, as with rapidly shortening or relaxed myofibrils.

MATERIALS AND METHODS

S1 and Cross-Linked Myofibril Preparations

S1[1] was prepared from rabbit white muscles of the back and pelvic limbs as described previously (*24*), stored at 4 °C, and used within 5 days.

Myofibrils were prepared from rabbit psoas muscle as described by Herrmann and co-workers (*23*) and stored at 4 °C for up to 3 days in storage buffer [50 mM Tris-acetate (pH 7.4), 100 mM potassium acetate, 5 mM KCl, 2 mM magnesium acetate, 2 mM DTT, 0.5 mM sodium azide, 0.2 mM PMSF, 10 μM leupeptin, and 5 μM pepstatin]. The standard cross-linking procedure was as described previously (*23*). Briefly, myofibrils were washed twice in cross-linking buffer [100 mM MES (pH 7.0), 3 mM magnesium acetate, and 3 mM EGTA] and incubated at a concentration of 10 mg/mL with 2 mM EDC and 5 mM NHS at 4 °C for 90 min. The cross-linking process was stopped by addition of 25 mM glycine and 10 mM DTT. To eliminate residual shortening which remains with this standard procedure (see the Results), in most experiments the cross-linking time was increased to 120 min. For subsequent experiments, the cross-linked myofibrils were washed twice in the appropriate buffer and filtered through a 149 μm mesh polypropylene filter to eliminate aggregates. The cross-linked myofibrils were used within 3 h of preparation. When they are left longer, especially at temperatures above 15 °C, cross-linked myofibrils tend to aggregate and are difficult to disperse. Native myofibrils only behaved in this way if left for several hours at higher temperatures.

The myosin head concentration in the myofibrillar suspension was measured by absorption at 280 nm (*25*).

Experimental Conditions

Unless otherwise stated, experiments were carried out at 20 °C. Experimental buffers were 50 mM Tris-acetate (pH 7.4), 100 mM potassium acetate, 5 mM KCl, and either 0.1 mM $CaCl_2$ and 2 mM magnesium acetate (activating buffer, with added Ca^{2+}) or 2 mM EGTA and 5 mM magnesium acetate (relaxing buffer, without Ca^{2+}).

Kinetic Studies

These studies were carried out either under single-turnover conditions, i.e., [myofibrils] > [ATP], or under multiturnover conditions where [myofibrils] < [ATP]. There were three types of experiment: P_i burst, cold ATP chase (by rapid flow quench), and fluorescence stopped flow. The data obtained were fitted using GraFit (Erithacus Software Ltd.).

P_i Burst Experiments. This type of experiment allows the measurement of the kinetics of formation of *total P_i*, i.e., free P_i and bound P_i [in Scheme 1, P_i with (A)M**·ADP·P_i and (A)M*·ADP·P_i]. They were carried out in a homemade, thermostatically controlled, rapid flow quench apparatus (*26*). With this apparatus, it took 10−15 min to obtain a time course with reaction mixtures of ages 200 ms to tens of seconds. The procedure was to mix myofibrils with [γ-^{32}P]-ATP in the apparatus. The reaction mixtures were quenched in acid (22% TCA and 1 mM KH_2PO_4) and the total P_i concentrations determined by the filter paper method of Reimann and Umfleet (*27*).

Cold ATP Chase Experiments. This type of experiment allows the measurement of the kinetics of formation of *tightly bound ATP* states [in Scheme 1, (A)M*·ATP] in addition to the total amount of P_i. The procedure was the same as that for P_i burst experiments except that the reaction mixtures were first quenched with a large molar excess of cold ATP [20 mM nonradioactive MgATP (pH 7.0)]. After incubation for 2 min on ice, the quenched reaction mixtures were stopped in acid and the amount of [^{32}P]P_i was determined. In these experiments, since in Scheme 1 step 2 is essentially irreversible, one obtains a transient phase of tightly bound ATP with kinetics of $k_{obs} = k_2[ATP]/(K_1 + [ATP])$ and an amplitude equal to the ATPase site concentration. Thus, in cold ATP chase experiments, one can titrate ATPase sites in myofibrils.

Fluorescence Stopped Flow Experiments. This type of experiment allows the measurement of the kinetics of *free P_i* release. They were performed in a Hi-Tech Scientific (Salisbury, U.K.) fluorescence stopped flow apparatus (model SF-61 DX2). The method is based on the increase in fluorescence of a phosphate binding protein labeled at an introduced cysteine with a coumarin derivative (MDCC-PBP; *11*) upon binding of P_i. The procedure was to mix a

[1] Abbreviations: DTT, dithiothreitol; EDC, 1-ethyl-3-[3-(dimethylamino)propyl]carbodiimide; EDTA, (ethylenedinitrilo)tetraacetic acid; EGTA, ethylene glycol bis(β-aminoethyl ether)-*N*,*N*,*N*′,*N*′-tetraacetic acid; MDCC-PBP, A197C mutant of the phosphate binding protein labeled with *N*-[2-(1-maleimidyl)ethyl]-7-(diethylamino)coumarin-3-carboxamide; MES, 2-(*N*-morpholino)ethanesulfonic acid; NHS, *N*-hydroxysulfosuccinimide; PMSF, phenylmethanesulfonyl fluoride; S1, myosin subfragment 1; Tris, tris(hydroxymethyl)aminomethane; XMF60, XMF90, and XMF120, myofibrils cross-linked with EDC for 60, 90, and 120 min, respectively.

suspension of myofibrils, containing MDCC-PBP, with a solution of ATP containing the same concentration of MDCC-PBP and to record the fluorescence increase kinetics. The fluorescent signal emitted by MDCC-PBP upon P_i binding was calibrated by mixing a known concentration of P_i (0−5 μM) to a solution of MDCC-PBP (with or without myofibrils or S1). The excitation wavelength was 436 nm, and emission wavelengths were >455 nm using a cutoff filter (GG455 from Hi-Tech). In certain experiments, to reduce traces of contaminant P_i, a P_i mop system was added to the experimental buffer. This system consists of 0.05 unit/mL purine nucleoside phosphorylase and 200 μM 7-methylguanosine (*11*). For each experiment, a series of 3−12 shots were carried out and averaged.

Sarcomere Length Measurements

To check the extent of residual shortening after cross-linking, myofibrils (at a concentration of 8 μM in myosin heads) in activating buffer were incubated at 20 °C with 100 μM ATP in a rapid flow quench apparatus and quenched at different times (from 0.2 s to 10 min) with 10 mM EDTA and 2 mM EGTA (pH 7.4). Sarcomere lengths were measured by transmitted light microscopy using a DMR B microscope (Leica, Germany), tube factor 1.6×, with a PL APO 100× immersion oil objective (NA 1.40). The images thus obtained were captured with a MicroMax 1300 Y/HS (B/W) cooled (−10 °C) CCD camera as 8 bit images (C mount 1×) and the MetaMorph (version 4.6r5) controller program (Princeton Instruments) run by a PC compatible microcomputer. The images were saved as TIFF images in 8 bit format. Sarcomere lengths were measured with Matrox Inspector 2.2 image processing software (Matrox Electronic Systems Ltd.). For each experimental condition, 10−20 myofibrils were analyzed and their sarcomere lengths averaged. The sarcomere lengths of cross-linked myofibrils (XMF90 or XMF120; see below) were in the range of 2.5−2.7 μm; i.e., the overlaps were at least 89% (*28*), as for uncross-linked myofibrils.

Force Measurements

Force developed by myofibrils (native and cross-linked, prepared as described above) was measured following the procedure of Colomo and co-workers (*29*). Briefly, myofibrils bathed in rigor (no ATP, low calcium) or relaxing (5 mM ATP, 1 mM free Mg^{2+}, pCa 8.0) solutions were attached to glass microtools at 20 °C. One of the microtools acted as a cantilever force probe of known compliance whose movement during contraction was followed by a photoelectronic device. Myofibrils were maximally activated and relaxed by rapidly translating (10 ms) the interface between two continuous streams of relaxing (pCa 8.0) and activating (pCa 4.5) solutions. All concentrations were calculated as described previously (*30*), and the final ionic strength was 200 μM (pH 7).

RESULTS

Attempts To Ensure Fully Isometric Contraction in Myofibrils

Shortening Experiments. In our previous work (*23*), we chose a cross-linking procedure that gave myofibrils that upon the addition of ATP did not "overcontract" [as uncross-linked myofibrils do (*20*, *31*)] and whose steady state rate of ATP hydrolysis was linear [i.e., no "break" as with rapidly shortening myofibrils (*31*)]. However, upon closer inspection, when ATP was added to these myofibrils, the sarcomeres shortened somewhat (typically ∼190 nm or 7.5%, at 100 μM ATP, under the microscope), but even after long incubation periods (several minutes at room temperatures at millimolar ATP concentrations) overcontraction did not occur. This shortening appeared to depend on the ATP concentration because it was more extensive at 1 mM than at 50 μM; it could lead to false transients as shortening myofibrils have a higher ATPase rate than myofibrils that are prevented from shortening (*23*). We made attempts to eliminate it with a more extensive cross-linking procedure and also by preincubating the cross-linked myofibrils with ATP before the kinetic experiments.

Table 1: Effects of the Extent of Cross-Linking on the Steady State Parameters of Myofibrils in Activating Buffer[a]

			at 4 °C		at 20 °C	
type of myofibril	incubation time (min)	% myosin heads cross-linked[b]	k_{cat} (s^{-1})	K_m (μM)	k_{cat} (s^{-1})	K_m (μM)
native[c]	0	0	1.7	8	8.3	14
XMF90[b]	90	6.5 ± 0.5	0.8	10	3.5	nd[d]
XMF120	120	8.0 ± 0.5	0.5	30	2.3	55

[a] From P_i burst experiments (e.g., Figure 2). The buffer was of 50 mM Tris, 100 mM potassium acetate, 5 mM KCl, 2 mM magnesium acetate, and 0.1 mM $CaCl_2$ (pH 7.4) (acetic acid). [b] From ref *23*. [c] From ref *18*. [d] Not determined.

Previously, we cross-linked myofibrils with EDC for 90 min, and we now increased this to 120 min. In these myofibrils, the sarcomeres shortened considerably less (∼65 nm or 2.6% at 100 μM ATP), possibly because more of the heads had been cross-linked (Table 1). We term these myofibrils "cross-linked myofibrils 90" (XMF90) and "cross-linked myofibrils 120" (XMF120).

We studied the residual shortening with XMF120 by quenching reaction mixtures (8 μM XMF120 and 100 μM ATP) of different ages in EDTA and EGTA and then measuring the sarcomere lengths of the myofibrils in the quenched reaction mixtures (Materials and Methods; result not illustrated). Because the shortening was limited and fast, it was difficult to obtain its kinetics, but it was over by 250 ms.

To reduce further any residual shortening during the kinetic experiments, we preincubated XMF120 with ATP. Typically, myofibrils (3 μM as myosin heads) were incubated with 1 mM ATP at 20 °C for 5 min. This allowed any residual shortening to occur and the total hydrolysis of the ATP. The myofibrils were then washed with buffer to remove ADP and P_i (as in Materials and Methods). Unfortunately, myofibrils pretreated with ATP were contaminated with P_i that interfered with the MDCC-PBP method. Extensive washing led to a degradation of the myofibrillar structure (as seen under the microscope). Therefore, we did not use this preincubation procedure in our experiments, and the myofibrils were cross-linked and washed as described in Materials and Methods.

Force Measurements. We checked if cross-linked myofibrils were still able to generate force. The effect of cross-linking time on force development and force decay are shown in Figure 1. The force measured with cross-linked myofibrils

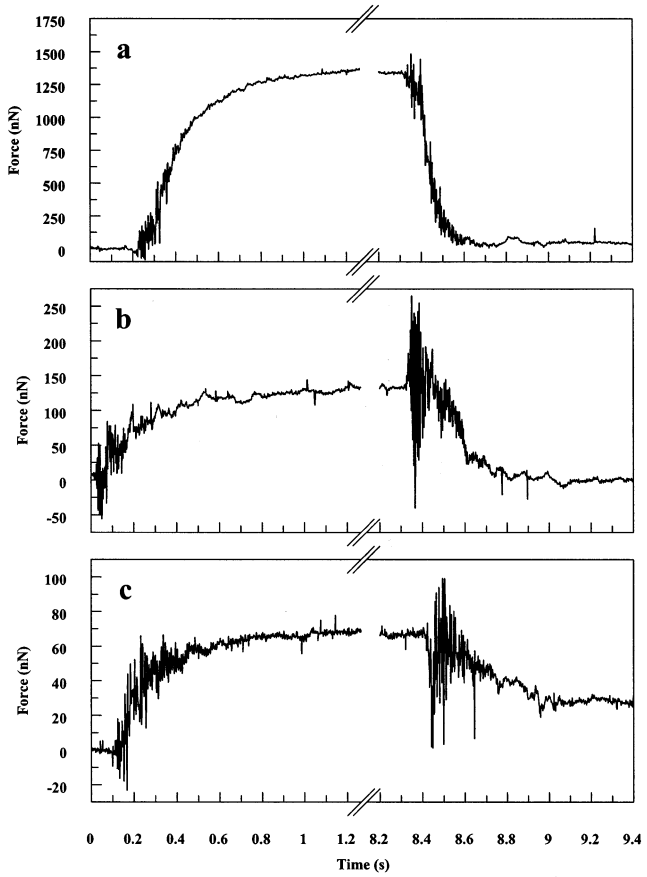

FIGURE 1: Force development upon addition of Ca^{2+} and force decay upon Ca^{2+} removal at 15 °C with (a) un-cross-linked myofibrils or myofibrils cross-linked for (b) 60 or (c) 120 min. The ATP concentration was 5 mM. For experimental details, see Materials and Methods. (a) Native myofibril [sarcomere length (sl) = 2.48 μm], maximal force = 1340 nN, k_{ACT} = 5.9 s^{-1}, clearly biphasic relaxation; (b) XMF60 (sl = 2.48 μm), maximal force = 128 nN, k_{ACT} = 5.6 s^{-1}; and (c) XMF120 (sl = 2.70 μm), maximal force = 69 nN, k_{ACT} = 5.8 s^{-1}, clearly monophasic relaxation.

was very small, as expected as the cross-linking procedure almost completely prevents shortening (especially XMF120). For this reason, force records with cross-linked myofibrils are very noisy, and they can only be interpreted qualitatively.

The kinetics of force development (k_{ACT}) appeared not to be greatly affected by the cross-linking procedure: k_{ACT} = 6.45 ± 0.78 s^{-1} (n = 2) for native myofibrils and 8.50 ± 2.84 s^{-1} (n = 5) for XMF120. The value of k_{ACT} obtained here with native myofibrils is in good agreement with the previously reported value [6.6 ± 1.5 s^{-1} (n = 29) (*32*)]. Interestingly, cross-linking seems to induce a progressive loss of the biphasicity of the relaxation phase previously observed in native myofibrils (R. Stehle et al. and C. Tesi et al., unpublished results). With extensively cross-linked myofibrils (XMF120), only the slow isometric phase was observed, as expected for a truly isometric preparation. Therefore, the force measurements confirm that the overall mechanical properties of the myofibrils are not affected by the cross-linking procedure and that XMF120 is a viable model for a fully isometric preparation.

Rapid Flow Quench Experiments

Cold ATP Chase and P_i Burst Experiments in the Steady State. Herrmann and co-workers (*23*) showed that at 4 °C

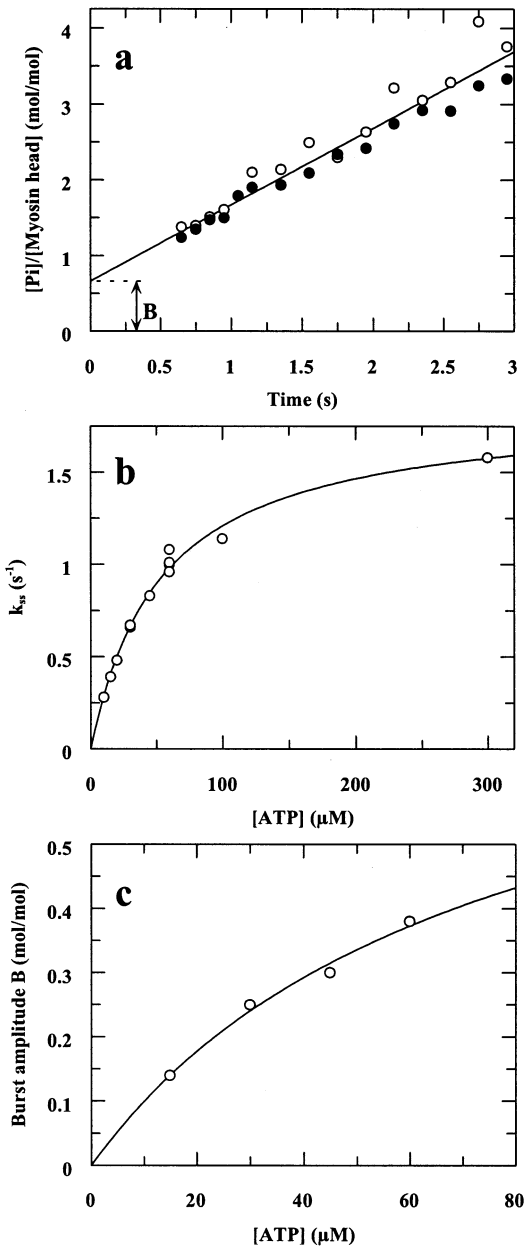

FIGURE 2: Multiturnover time courses for total P_i formation in cold ATP chase (○) and P_i burst (●) experiments with XMF120 in activating buffer at 20 °C. (a) The reaction mixtures (6 μM as myosin heads and 60 μM [γ-^{32}P]ATP) were quenched either directly in acid (●) or first in 50 mM unlabeled ATP for 2 min (on ice) and then in acid (○). Finally, the amount of [^{32}P]P_i was determined. The data were fitted to a transient burst phase with an amplitude B of 0.66 mol of total P_i/mol of myosin heads followed by a steady state rate k_{ss} of 1.01 s^{-1}. (b) Dependence of k_{ss} in P_i burst experiments on the ATP concentration. The data were fitted to a hyperbola giving a k_{ss}^{max} of 1.9 s^{-1} and a K_m of 55 μM. (c) Dependence of B in P_i burst experiments on the ATP concentration. The data were fitted to a hyperbola giving a B^{max} of 0.83 mol/mol and a K_d of 73 μM. The experimental conditions are in Materials and Methods.

cold ATP chase and P_i burst time courses with XMF90 were identical, and they suggested that $K_3 \geq 10$ (Scheme 1), as with un-cross-linked myofibrils (*19*, *25*). Here we confirmed this similarity with XMF120 at 20 °C. Thus, in Figure 2a, the two time courses were indistinguishable, with a transient burst phase with an amplitude B of 0.66 mol of P_i/mol of myosin head and a steady state rate k_{ss} of 1.0 s^{-1}. The effect

of the concentration of ATP on these steady state parameters is illustrated in panels b and c of Figure 2, and the values obtained are given in Table 1, which also includes those at 4 °C. In the table, k_{cat} refers to k_{ss} at high ATP concentrations (k_{ss}^{max}, Figure 2b) and corrected for the active site concentration as obtained from the transient P_i burst amplitude at saturation in ATP (B^{max}, Figure 2c). We note that for XMF120 the k_{cat} is lower and the K_m higher than for XMF90.

Our estimates of the steady state parameters for XMF120 agree well with those obtained by Glyn and Sleep (*33*), also for EDC cross-linked myofibrils: at 15 °C, 0.8 s^{-1} for the steady state rate and 15.7 μM for the K_m.

The sensitivity of the steady state parameters to the ATP concentration is noteworthy as it suggests that in the concentration range of ATP that was used, intermediates containing ADP·P_i, rather than ADP, predominate on the myofibrillar ATPase pathway.

Estimation of the Equilibrium Constant for the Cleavage Step K_3. With S1 and if Scheme 1 is assumed (without actin), K_3 is estimated from the ratio of the amplitudes of the transients in cold ATP chase [B_{ch} = ATPase site/myosin head (mole per mole)] and P_i burst (B_{P_i}) experiments. Thus, $B_{P_i}/B_{ch} = K_3/(1 + K_3)$, or $B_{P_i}/(B_{ch} - B_{P_i}) = K_3$. Typically, S1 titrates 0.7 mol of site/mol of S1 protein (B_{ch}) and $B_{P_i} = 0.5$ mol of P_i/mol of S1 protein. Therefore, $K_3 = 2.5$. With XMF120 and from Figure 2a, $B_{P_i}/B_{ch} \sim 1$. Therefore, if it is assumed that Scheme 1 applies to the myofibrillar ATPase, with XMF120 $K_3 \geq 10$. However, as discussed below, Scheme 1 may not be adequate to describe the ATPase of XMF120.

Kinetics of the P_i Burst Transient with XMF120. To confirm a transient burst phase, its kinetics should be obtained. With myofibrils, this needs a rapid quench flow apparatus designed to work in the time range of 4−400 ms. However, with this apparatus, it was difficult to work at XMF120 concentrations of >1 μM (i.e., [ATP] > 10 μM) and at temperatures above 15 °C; clogging of the mixers and aggregation of the myofibrils during the experiment occurred because with this apparatus it takes ~1 h to obtain a time course.

A time course for the ATPase of XMF120 at 12 °C is shown in Figure 3, with 1 μM XMF120 and 10 μM [γ-^{32}P]-ATP. The time course was biphasic: an initial burst that is followed immediately by a steady state phase. With the caveat that this experiment was carried out at 12 °C, it confirms that the P_i bursts obtained in Figure 2 are manifestations of ATPase intermediates. We note that had the ADP release kinetics (k_6 in Scheme 1) been rate-limiting, i.e., $k_3 + k_{-3} > k_4 > k_6$, the time course could have been triphasic: a rapid P_i transient of kinetics directed by k_2/K_1 and $k_3 + k_{-3}$, a second transient of kinetics directed by k_4, and finally a steady state directed by k_6. This was the case with S1 under cryoenzymic conditions (−15 °C) (*34*).

Single-Turnover Experiments. A key feature of myosin head ATPase, whether in S1, acto-S1, or un-cross-linked myofibrils, is that the ATP is bound essentially irreversibly, i.e., $k_{-2} \ll k_o \ll k_2$, where $k_o = k_4K_3/(1 + K_3)$ (Scheme 1; ref *23* and references therein). This could explain the low K_m for ATP with un-cross-linked myofibrils and especially S1. Therefore, the higher K_m with XMF120 (Table 1) could be a reflection of a weaker ATP binding, i.e., a higher value for k_{-2}. A sensitive test for tight ATP binding is to carry

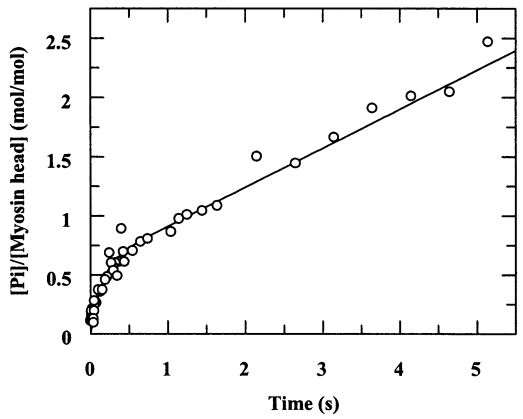

FIGURE 3: Kinetics of the total P_i transient with XMF120 in activating buffer at 12 °C. The reaction mixtures (1 μM XMF120 and 10 μM [γ-^{32}P]ATP) were quenched in acid at the times indicated, and the amount of [^{32}P]P_i was determined. The data were fitted to a P_i burst transient with an amplitude of 0.58 mol of total [^{32}P]P_i/mol of myosin heads and a k_{obs} of 6.9 s^{-1} followed by a steady state rate of 0.33 s^{-1}.

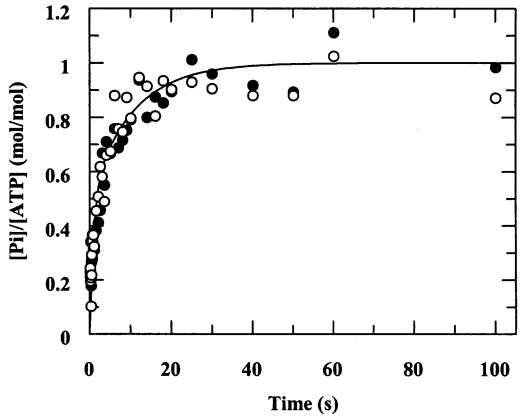

FIGURE 4: Single-turnover ATP chase time courses with XMF120 in activating buffer at 20 °C. The reaction mixtures [(●) 3 μM XMF120 and 1 μM [γ-^{32}P]ATP and (○) 3 μM XMF120 and 0.3 μM [γ-^{32}P]ATP] were quenched in cold ATP at the indicated times, and the amount of [^{32}P]P_i was determined. For further details, see Materials and Methods. The data were fitted to two exponentials with a final amplitude of ≥0.98 mol of [^{32}P]P_i/mol of [γ-^{32}P]ATP ($Ampl_1$ = 0.5 mol/mol, k_{obs1} = 1.12 s^{-1}, $Ampl_2$ = 0.5 mol/mol, k_{obs2} = 0.10 s^{-1}).

out cold ATP chase experiments under single-turnover conditions because in these one measures the ratio of k_{-2} (ATP off as ATP) to k_o (ATP off as ADP + P_i). Single turnovers should be carried out at both low and high [myosin heads] to [ATP] ratios. Thus, at a high ratio, a rare, atypical site could bind selectively all of the little ATP present, leading to misleading kinetics.

The results of single-turnover chase experiments with XMF120 at different ratios of heads to ATP, but at the same concentration of XMF120 (3 μM), are shown in Figure 4. There are three features of these experiments. First, the time courses were very similar, and the data were combined. Second, there was a rapid rise of P_i of amplitude of ≥0.98 mol of [^{32}P]P_i/mol of [γ-^{32}P]ATP. Finally, the rapid rise was biphasic. Biphasic ATP chase single turnovers were also obtained with un-cross-linked myofibrils, acto-S1, and S1 and may be due to two types of sites for ATP: a site that hydrolyzes ATP by the Bagshaw−Trentham mechanism and a site where the ATP is trapped transiently without being

hydrolyzed. Here we did not investigate further this phenomenon; for a full discussion, the reader is referred to ref *25* and references therein. The important conclusion from Figure 4 is that the $^{32}P_i$ in [γ-^{32}P]ATP was recovered almost completely as [^{32}P]P_i; because the amplitude $= k_o/(k_o + k_{-2}) \geq 0.98$, $k_o \gg k_{-2}$ which shows that ATP binds as tightly to XMF120 as to the other muscle systems that were studied.

With S1 ATPase, *P_i burst single turnovers* aid in assigning the rate-limiting step. Thus, on the $1/k_{cat}$ time scale (tens of seconds), total P_i time courses consist of a rapid rise of amplitude $K_3/(1 + K_3)$ followed by a slow exponential that leads to the complete hydrolysis of the ATP with kinetics $k_o = k_4K_3/(1 + K_3)$ (refs *24* and *35* and references therein). Thus with Scheme 1, single turnovers lead directly to K_3 and k_4.

With S1 at 20 °C, $k_o = k_{cat}$ which shows that the P_i release step is rate-limiting; i.e., if Scheme 1 is assumed, the M**·ADP·P_i state accumulates in the steady state. At low temperatures (*36*, *37*), particularly under cryoenzymic conditions (*38*), the ADP kinetics are rate limiting and $k_o > k_{cat}$; i.e., the M*·ADP state accumulates in the steady state.

However, with Ca^{2+}-activated or cross-linked myofibrils, P_i burst single turnovers are less informative. First, because if $K_3 \geq 10$, the amplitude $[1/(1 + K_3)]$ of the phase giving k_o is small; second, unless high concentrations of myofibrils are used, $k_o \cong k_{obs}$ (kinetics of the fast, initial phase which are a function of $k_3 + k_{-3}$ and k_2/K_1) so the two phases would not be separated clearly anyway (see ref *19* for relaxed myofibrils).

Effect of P_i on the ATPase of Cross-Linked Myofibrils at 20 °C. Were the (A)M·ADP states to predominate in the steady state, added unlabeled P_i should decrease the level of these states and k_{ss}. We carried out three steady state experiments with the same XMF120 solution and on the same day, as in Figure 2a: no P_i, $k_{ss} = 1.08\ s^{-1}$; 0.5 mM P_i, $k_{ss} = 0.92\ s^{-1}$; and 5 mM P_i, $k_{ss} = 1.04\ s^{-1}$. Thus, P_i had little effect on the k_{ss} of XMF120, as found previously with un-cross-linked myofibrils (*39*). This suggests that the transient P_i burst is due to (A)M·ADP·P_i states rather than free P_i. Pate and Cooke (*40*) found that P_i had little effect on the isometric ATPase of muscle fibers.

Affinity of Cross-Linked Myofibrils for MgADP. S1 has a strong affinity for ADP [$K_d \sim 1\ \mu$M (*35*)] that can be explained by a slow k_{off} (k_6 in Scheme 1). Thus, with S1 at temperatures around 4 °C, $k_{cat} \sim k_o \sim k_6$ (*35*). Acto-S1 and un-cross-linked myofibrils have a much weaker affinity for ADP ($K_d \sim 150\ \mu$M; *39*, *41*, *42*) which is explained by a fast k_6 (*4*, *34*), i.e., $k_6 \gg k_{cat}$. With cross-linked acto-S1, $k_{cat} \sim k_3 + k_{-3}$ (*43* and references therein), and with native myofibrils, $k_{cat} \sim k_o \sim k_4$ (*21*).

Here, we determined the affinity of cross-linked myofibrils for ADP by the method of Sleep and co-workers (*44*), i.e., by determining the effect of ADP upon the ATP binding kinetics (k_2/K_1) in single-turnover P_i burst experiments at low concentrations of myofibrils and, of course, ATP. The K_d value that was obtained, $250 \pm 50\ \mu$M (Figure 5), is reasonably close to that for un-cross-linked myofibrils [140 μM (*44*)] which suggests that also with cross-linked myofibrils $k_6 \gg k_{cat}$, i.e., that (A)M·ADP·P_i states accumulate in the steady state. However, this argument does not take account of the A-M′·ADP intermediate of Sleep and Hutton (*45*) (Scheme 2) which is only formed from ATP. Thus, the possibility that, with ATP, the ADP release kinetics are directed by the kinetics of step a of Scheme 2 rather than k_6 cannot be excluded.

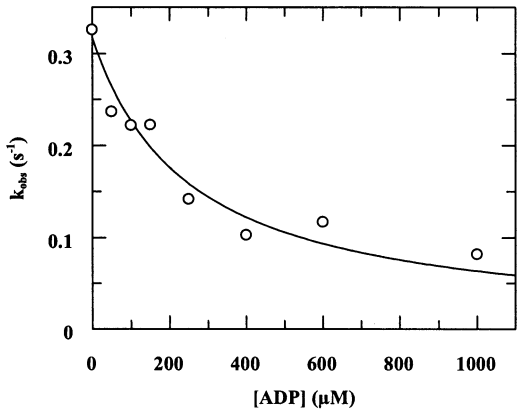

FIGURE 5: Dependence of the single-turnover P_i burst kinetics (k_{obs}) on the ADP concentration at 20 °C. The reaction mixtures included 3 μM XMF120, 0.6 μM [γ-^{32}P]ATP, and different ADP concentrations. For full details, see ref *44*.

Scheme 2

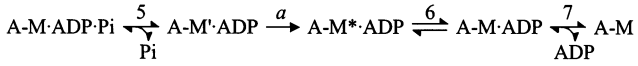

Conclusions. With myofibrils, the single-turnover P_i burst method could not be used to measure specifically the kinetics of P_i release. Nevertheless, taken together, the results of the rapid flow quench experiments suggest strongly that the predominant intermediates on cross-linked myofibrillar ATPase are (A)M·ADP·P_i states, as with native relaxed and Ca^{2+}-activated myofibrils. To confirm, we now carried out experiments in which free P_i [by implication (A)M·ADP states] was determined specifically.

Fluorescence Stopped Flow Experiments

Because our aim was to determine whether there are genuine free P_i transients with cross-linked myofibrillar ATPase, we carried out several control experiments.

First, we checked on the calibration of the MDCC-PBP system in the presence of cross-linked myofibrils. Second, to check our stopped flow apparatus and the suitability of our experimental conditions, we carried out free P_i measurements on the well-studied S1 ATPase. S1 ATPase is a good control for the MDCC-PBP method because at >10 °C the P_i release kinetics are rate-limiting so free P_i progress curves should be linear without a transient phase. Free P_i measurements by the MDCC-PBP method do not appear to have been carried out on S1 ATPase under multiturnover conditions.

Calibration. Two methods were used. In the first, MDCC-PBP and P_i were mixed with the P_i mop in a stopped flow apparatus and the decrease in fluorescence was measured. The concentrations (in the mixture) were typically 5 μM MDCC-PBP and 1 μM P_i which resulted in a decrease in fluorescence when the P_i mop was added (see Materials and Methods).

The second method is more rigorous. Here, the MDCC-PBP is titrated with P_i, as in Brune et al. (*46*). We found that with 5 μM MDCC-PBP, the fluorescence increased

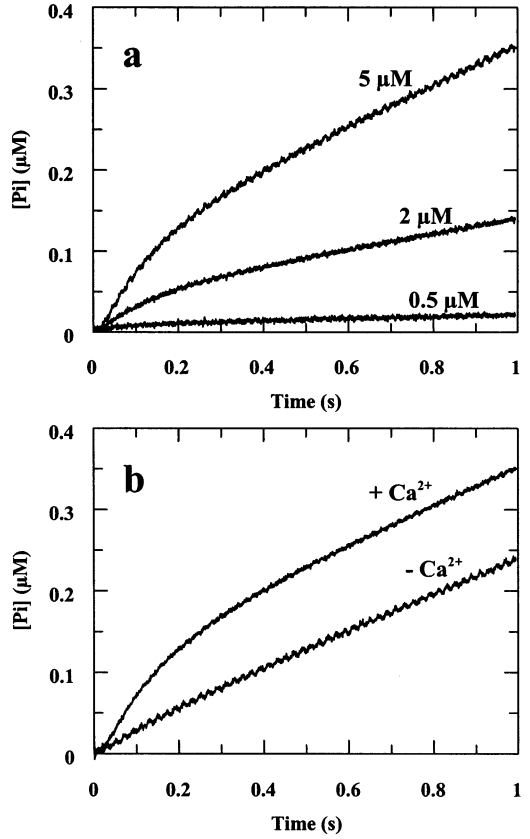

FIGURE 6: Time course of free P_i formation with S1 ATPase at 20 °C. The amount of P_i was measured by fluorescence stopped flow using MDCC-PBP. In panel a, the reaction mixtures contained P_i mop, 5 μM MDCC-PBP, 30 μM ATP, and 0.5, 2, or 5 μM S1. Each time course (at 2 and 5 μM S1) was fitted to an initial phase with an amplitude of 0.024 mol of P_i/mol of S1 and a steady state rate k_{ss} of 0.048 s^{-1} for 2 μM S1 and a k_{ss} of 0.050 s^{-1} for 5 μM S1. The buffer contained 0.1 mM $CaCl_2$. In panel b, the reaction mixtures (P_i mop, 5 μM MDCC-PBP, 30 μM ATP, and 5 μM S1) contained no or 0.1 mM $CaCl_2$. Note that the data are expressed as the concentration of free P_i. For further details, see Materials and Methods.

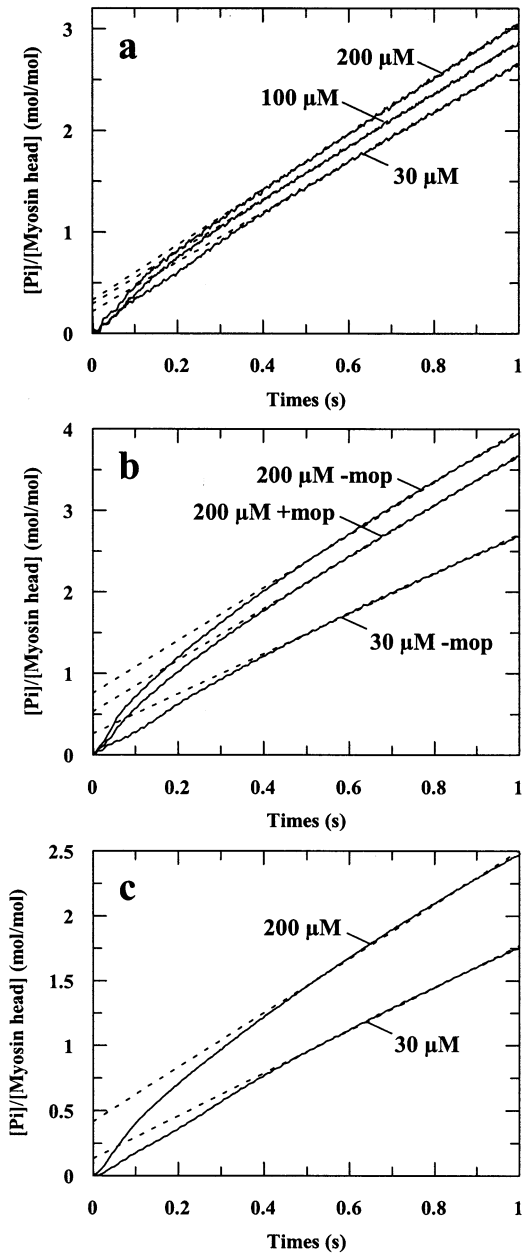

FIGURE 7: Time courses of free P_i formation with XMF90 at 20 °C. The amount of P_i was measured by fluorescence stopped flow using MDCC-PBP. The concentrations were as follows: (a) 0.5 μM XMF90, 20 μM MDCC-PBP, and 30, 100, or 200 μM ATP, (b) 1 μM XMF90, 20 μM MDCC-PBP, and 30 μM ATP (no mop) or 200 μM ATP (with or without mop), and (c) 2 μM XMF90, 20 μM MDCC-PBP, and 30 or 200 μM ATP.

linearly with the P_i concentration up to ~1.5 μM P_i. At higher P_i concentrations, the fluorescence increased nonlinearly, reaching a plateau at 3.5−4.5 μM P_i, depending on the batch of MDCC-PBP, in agreement with previous results (*46*). This lack of linearity could explain the curved myofibrillar ATPase time courses sometimes obtained by the MDCC-PBP method as compared with the linear time courses obtained by chemical sampling (*21*, *22*). Therefore, with 5 μM MDCC-PBP, we limited our measurements to 1.5 μM P_i. For higher P_i concentrations, we increased the MDCC-PBP concentration.

The presence of S1 (5 μM) or cross-linked myofibrils (1 μM) had little effect on the P_i titration curves. With myofibrils there was a small increase in the magnitude of the fluorescence signal due to turbidity, but this did not affect the calibration.

Experiments with S1. Typical time courses with S1 at different concentrations are illustrated in Figure 6a. It is noteworthy that at 2 μM and especially 5 μM S1 there were transient fluorescent phases that preceded the steady state phases. The steady state rates (0.048 and 0.050 s^{-1}, respectively) agreed well with that found by chemical sampling at 0.5 μM S1 (0.046 s^{-1}, time course not shown). These experiments were carried out in activating buffer, i.e., with 0.1 mM $CaCl_2$.

The amplitudes of the phases were very low (both 0.024 mol of P_i/mol of S1) and the kinetics difficult to fit to single exponentials. They are probably due to the Ca^{2+}-ATPase activity of S1, which is 2 orders of magnitude higher than the Mg^{2+}-ATPase activity because, as shown in Figure 6b, they were absent in the relaxing buffer (i.e., in the presence of EGTA). These experiments illustrate the sensitivity of the MDCC-PBP method to P_i transients and the care needed to eliminate spurious phases.

Experiments with XMF90. Free P_i progress curves with XMF90 at 30, 100, and 200 μM ATP are shown in Figure 7a. Each curve consists of an initial rapid phase that is

followed by a slower, apparently linear phase. The *amplitudes* of the initial phases were large (0.22−0.33 mol of P_i/mol of myosin heads), but the *kinetics* could not be fitted to exponentials. It is noteworthy that the phases occurred on the same time range as the residual shortening mentioned above.

The final linear phases fitted well to the steady state ATPase obtained in rapid flow quench experiments: at 30 μM ATP 2.45 s^{-1} by stopped flow compared to 2.6 s^{-1}, at 100 μM ATP 2.58 s^{-1} compared to 3.2 s^{-1}, and at 200 μM ATP 2.73 s^{-1} compared to 3.3 s^{-1}.

The results of further experiments on different myofibrillar preparations revealed that the amplitudes of the initial phases were not reproducible (from 0.13 to 0.76 mol of P_i/mol of myosin heads), as illustrated in panels b and c of Figure 7. The phases were not detected in rapid flow quench experiments because the first sampling times were later (0.2−0.3 s), but clearly, the magnitudes of P_i burst or cold ATP chase amplitudes with XMF90 must be interpreted with caution.

An explanation for the initial fast phase is that it is a manifestation of the higher ATPase due to the "residual" sarcomere shortening mentioned above. To put this explanation to the test, we now carried out P_i measurements with myofibrils that had been more extensively cross-linked, i.e., in which the residual shortening had been reduced.

Experiments with XMF120. As illustrated in Figure 8a, with the more heavily cross-linked XMF120, there still was an initial free P_i transient but its amplitude was only $^1/_{10}$ of that with XMF90. In a rapid flow quench experiment and at the same concentration of ATP (100 μM), there was a large P_i burst of total P_i with an amplitude of 0.55 mol of P_i/mol of myosin heads. The two steady state rates agreed reasonably well: 1.14 s^{-1} for free P_i and 1.6 s^{-1} for total P_i.

Free P_i progress curves on a shorter time scale and at three concentrations of XMF120 are illustrated in Figure 8b. Each P_i progress curve consists of a small fast phase (at 1 μM myofibrils, amplitude = 0.033 mol of P_i/mol of myosin heads and at 2 and 4 μM, 0.009 mol/mol) that is followed by a linear phase representing the steady state rate of ATP hydrolysis (k_{ss} = 1.14, 1.06, and 0.76 s^{-1}, respectively). It is noteworthy that the transients were over before 250 ms, as found for the residual shortening mentioned above. The k_{ss} with 4 μM myofibrils is low possibly because of an earlier saturation of the MDCC-PBP with P_i.

These results suggest that the large, transient phases with XMF90 are due to the residual sarcomere shortening that has a relatively high ATPase activity. Thus, with cross-linked myofibrils, it appears that the predominant intermediates in the steady state are (A)M·ADP·P_i states and that the concentration of (A)M·ADP states is low.

Another noteworthy feature of the stopped flow traces is that with 2 and 4 μM XMF120 there were transient lag phases, as found with un-cross-linked myofibrils (*21*), that presumably are a manifestation of the buildup of (A)M·ADP·P_i states that are not measured in free P_i measurements.

The dependence of k_{ss} on the ATP concentration agreed well with that obtained by total P_i determinations. Thus, at 60 μM ATP k_{ss} = 1.07 s^{-1} (total P_i gave 1.04 s^{-1}), at 100 μM ATP 1.14 s^{-1} (1.27 s^{-1}), and at 300 μM ATP 1.49 s^{-1} (1.63 s^{-1}) (progress curves not illustrated).

In the absence of Ca^{2+} and at 100 μM ATP, the ATPase rate of XMF120 was 0.44 s^{-1} compared to a value of 1.14 s^{-1} with Ca^{2+} (Figure 8c). With XMF90, the k_{ss} was 0.29 s^{-1} without Ca^{2+} and 0.43 s^{-1} with Ca^{2+}, but at 4 °C. We note that the small initial fast phase was also obtained in the absence of Ca^{2+}.

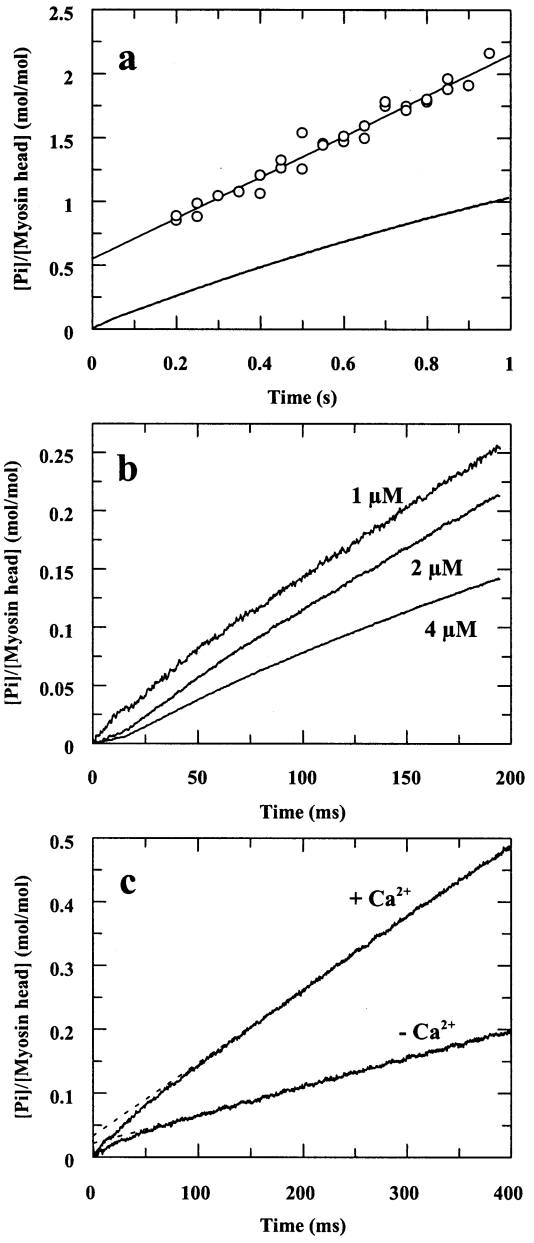

FIGURE 8: Time courses of free and total P_i formation with XMF120 at 20 °C. Unless otherwise stated, the buffer contained 0.1 mM $CaCl_2$. (a) The amount of P_i was measured by fluorescence stopped flow using MDCC-PBP (—) (reaction mixture of P_i mop, 5 μM MDCC-PBP, 1 μM XMF120, and 100 μM ATP). For the P_i burst experiment (reaction mixture of 10 μM XMF120 and 100 μM ATP), the data were fitted to a rapid transient phase with an amplitude of 0.55 mol of total P_i/mol of myosin heads followed by a k_{ss} of 1.6 s^{-1} (○). (b) Fluorescence transients at 1, 2, or 4 μM XMF120 and 100 μM ATP. (c) Fluorescence transients given by 1 μM XMF120 and 100 μM ATP in the presence or absence of Ca^{2+}. The kinetic constants that were obtained are in the text.

Conclusions. After an evaluation of the MDCC-PBP method with cross-linked myofibrils under our experimental conditions, to eliminate spurious phases, free P_i measurements with myofibrils (in which 6.5% of the heads had been cross-linked to the thin filament) gave large and rapid phases that were followed by steady state phases of ATP hydrolysis.

The initial phase is almost certainly explained by a residual sarcomere shortening process because in more heavily cross-linked myofibrils (8% heads cross-linked) the phase was reduced greatly. Thus, it appears that with myofibrils that are prevented from shortening by chemical cross-linking, in XMF120, (A)M·ADP·P_i states predominate in the steady state, with (A)M·ADP states representing <5% of the myosin heads.

DISCUSSION

We show here that the predominant intermediates on the ATPase reaction pathway of myofibrils prevented from shortening are almost certainly (A)M·ADP·P_i states. Thus, with all mechanical conditions studied so far [relaxed, rapidly shortening (*21*), or isometric (this study)], (A)M·ADP·P_i states predominate. Also consider the biphasic ATPase of unheld, Ca^{2+}-activated myofibrils: a rapid k^F followed by a slow k^S (*39*). During the fast rate, the myofibrils shorten rapidly; when the sarcomeres reach 2.0−2.1 μm, both shortening and ATPase rates are reduced, presumably because the thin filaments now touch the M-lines. It has been suggested that k^S is the ATPase of myofibrils that are contracting isometrically (*47*). Therefore, had there been a change in the rate-limiting step in going from k^F (P_i release rate-limiting) to k^S (ADP release rate-limiting), there would have been a transient burst phase of free P_i at the k^F to k^S transition. Free P_i transients were not detected, so it appears that the (A)M·ADP·P_i states predominate for the duration of both k^F and k^S (*21*, *22*).

That (A)M·ADP·P_i states predominate with isometric myofibrils is at first sight difficult to reconcile with fiber and, in particular, myofibrillar mechanics because several workers suggest that in going from the rapidly shortening to the isometric condition, there is a switch in the rate-limiting step [P_i release (k_4 in Scheme 1) to ADP release (k_6)]. This conclusion comes from the sensitivity to P_i of isometrically held fibers (*8*, *9*, *40*) or single myofibrils (*32*, *48*). With an increase in P_i concentration, the isometric force decreased and the rate constant for force development increased, but the unloaded shortening velocity (V_{max}) and the overall ATPase rate were affected little. As the dependence of force on the P_i concentration was hyperbolic and the asymptote at infinite P_i concentration was not zero, a two-step mechanism was proposed (Scheme 3).

Clearly, to affect force development, P_i must interact with an A-M·ADP state, a state that we were unable to detect whether the myofibrils were shortening actively or held isometrically. A secondary allosteric site for P_i cannot be excluded, but there is little evidence for this.

How can we reconcile the chemical kinetic and mechanical data? What are the implications for the mechanochemical transduction in muscle contraction? First, we must consider the authenticity of cross-linked myofibrils as the isometric state.

Do Chemically Cross-Linked Myofibrils Mimic the Isometric State?

Although we cannot exclude entirely the possibility that the myofibrils had been affected adversely by the cross-linking procedure, we think that this is unlikely. First, the cross-linking procedure did not significantly affect the ATPase activity of S1 as determined by P_i burst and cold ATP chase experiments (*23*). Similarly, the procedure does not inhibit the actin activation of S1 ATPase whether the actin had been activated by EDC at 4 or 20 °C (P. Chaussepied, personal communication). Also, it does not significantly affect the ATPase sites of myofibrils (ref *23* and this study), as determined by the cold ATP chase method. The decrease in k_{cat} (Table 1) without affecting the ATPase site concentration can be explained by the Fenn effect (see below). Second, key features of the ATPase of un-cross-linked myofibrils remain with XMF120: $k_{-2} \ll k_{cat}$, apparent $K_3 \geq 10$, and similar K_d values for ADP. Third, the overall structure of the cross-linked myofibrils, including sarcomere lengths, could not be distinguished from those of un-cross-linked myofibrils (as seen under the microscope). Finally, as illustrated in Figure 1, the mechanical properties of XMF120 are those expected of the isometric condition.

Scheme 3

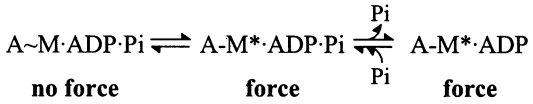

However, there is a caveat: cross-linked myofibrils are not fully regulated because whether Ca^{2+} is present, their ATPase activity is almost 2 orders of magnitude greater than that of relaxed native myofibrils. The high ATPase in the absence of Ca^{2+} is almost certainly a manifestation of rigor activation caused by the permanently linked bridges introduced by the cross-linking procedure. Although modification of the Ca^{2+}-regulation apparatus cannot be ruled out, there was no evidence for this from structural studies (*23*). Further, the myofibrils were to a certain extent activated by Ca^{2+}.

Models for Connecting the Mechanical and Chemical Kinetic Data with Cross-Linked Myofibrils (XMF120)

Our aim was to find the simplest possible model for accommodating the *chemical kinetic* data with cross-linked myofibrils (XMF120) and *mechanical data* with isometrically held myofibrils and fibers. In our search, we took into account the notion of duty cycle. Thus, it is thought that with skeletal fibers, the duty cycle for active myosin heads is low, i.e., that only a fraction of the myosin heads is attached and generates tension at any given time (*3*, *49*, *50*). This fraction is in the range 10−50%, and may depend on the method used and, possibly, the mechanical condition. By "attached" we mean myosin heads that are bound tightly to actin (e.g., as in A-M*·ADP·P_i or A-M*·ADP states, Scheme 3) and by "detached" heads that are bound weakly (e.g., A~M·ADP·P_i state, Scheme 3). The duty cycle is then given by the relative amounts of attached and detached heads.

A Model in Which Attached and Detached Heads Have Different Rate-Limiting Steps. Here, we assume that the *detached* heads hydrolyze ATP via rate-limiting P_i release, i.e., that (A)M·ADP·P_i states accumulate in the steady state and that the *attached heads* hydrolyze ATP via a rate-limiting ADP release step. With these, (A)M·ADP states accumulate. This two-pathway model, which is based on the work of Geeves and Holmes (*7*), Amitani et al. (*50*), and Tesi et al. (*32*), is given by Scheme 4 in which A-M represents strongly attached ("high force") and A~M weakly attached ("low force") states. The rate-limiting steps are in bold. Steps 2

Scheme 4

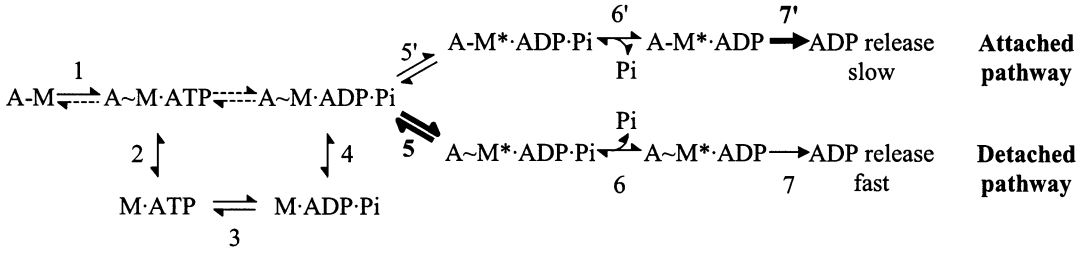

Scheme 5

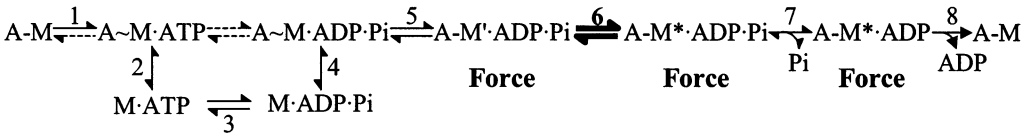

and 4 are rapid equilibria, steps 5 and 5′ relatively slow protein isomerizations, and steps 6 and 6′ diffusion-controlled processes. Steps 7 and 7′ are composite: relatively slow isomerizations followed by rapid releases of ADP. The rate-limiting step with the detached pathway is P_i release (kinetics directed by step 5) and with the attached pathway ADP release (step 7′).

This model requires a low duty cycle (≤5%) because the concentration of the strongly attached A-M*·ADP state is low (<0.05 mol/mol of myosin heads as judged by the free P_i measurements). Therefore, in Scheme 4 we propose that the attached pathway involves ≤5% and the detached pathway ≥95% of the heads. To ensure the efficiency of the contraction (*51*, *52*), we assume that the k_{ss} of the detached heads is low, possibly that of fully relaxed myofibrils (0.07 s^{-1} at 20 °C), and that the measured k_{ss} (2.3 s^{-1}) is due mostly to the attached heads. However, the P_i burst of ADP·P_i states is due almost entirely to the detached heads. To summarize, the total P_i burst transient is a reflection of the detached heads and the overall k_{ss} and mechanics of the attached heads. In this model, the ADP release kinetics are modulated by the mechanical state of the myofibrils, as postulated by Geeves and Holmes (*7*).

Although this model accommodates most of the chemical kinetic and mechanical data, it is not wholly satisfactory. First, if the overall k_{ss} were to be directed by the attached pathway with its important A-M*·ADP state, it would be sensitive to added P_i. However, the k_{ss} was insensitive to P_i (Results, above). Of course, it could be that in XMF120 the contraction is relatively inefficient, i.e., that the overall k_{ss} is a reflection of the detached rather than the attached pathway. Second, the model implies a rather low duty cycle (≤5%), but this could be because chemically cross-linked myofibrils have a lower duty cycle than isometric fibers. Third, to account for an overall k_{ss} of 2.3 s^{-1} which is due almost entirely to the 5% of heads that are attached, the ATPase of these few heads would be high (40−50 s^{-1}).

We now consider a model in which there is only one pathway.

A Model with Four (A)M·ADP·P_i States. Scheme 5 is an adaptation of the three-step P_i release scheme of Ranatunga (*53*) in which K_2 and K_4 are rapid equilibria. Because of the rapidity of the ATP binding kinetics (step 1), the concentration of the A-M state is low.

A key feature of this scheme is that the kinetics of a step immediately following a high force state are slow (step 6). Step 5 may also be relatively slow [as proposed by Ranatunga (*53*)] and may be the rate-limiting step in rapidly shortening myofibrils. The important point is that in the steady state both the low force A∼M·ADP·P_i and high force A-M·ADP·P_i states accumulate, the relative amounts depending on the equilibrium constant K_5. The transients in the P_i burst experiments are composed almost exclusively of these two states (with the M·ADP·P_i state). The concentration of the A-M*·ADP·P_i state is low because at low P_i concentrations step 7 is virtually irreversible. Consequently, in this model the duty cycle is mainly a function of K_5 and K_4.

In the mechanical experiments, when P_i is added, isometric force is reduced because step 7 becomes a rapid equilibrium and the system is shifted toward the low force A∼M·ADP·P_i state (and then M·ADP·P_i state, etc.). This implies that *k*-6 is large.

Which Model? From our experiments, it is difficult to choose between the two models. In the model in Scheme 4, there are two ATPase pathways: one for detached heads with P_i release being rate-limiting and the other for attached heads with ADP release being rate-limiting. In Scheme 5, there is only one pathway. To distinguish between Schemes 4 and 5, we need a method that selectively measures chemically the few attached heads in the presence of a large excess of detached heads.

The problem is also difficult because there is considerable evidence, both chemical kinetic and mechanic, that the myosin head ATPase pathway has several ATP states (*54*), ADP·P_i states (*53*), and ADP states (*45*), as predicted by the model of Geeves et al. (*55*) and by the structural analysis of Geeves and Holmes (*7*). This makes it difficult to assign chemical kinetic data to particular intermediate(s). For instance, in P_i burst experiments, the transient burst amplitude represents the sum of *all* ADP·P_i states (in Scheme 5) plus any free P_i. We discuss this further below. However, in certain mechanical experiments, the data can be assigned more precisely. Thus, the sensitivity of isometrically held fibers to P_i can be attributed to an interaction of P_i with the A-M′·ADP state of Sleep and Hutton (*45*), as given in Scheme 2. Any interaction of the A-M*·ADP or A-M·ADP state with P_i would presumably not lead to a mechanical signal as step a is essentially irreversible.

Do We Measure K_3, the Equilibrium Constant for the Cleavage Step, in P_i Burst Experiments? With S1, K_3 is obtained from the size of the amplitude of the transient in P_i burst experiments (*35*). In our previous work, we applied this method to myofibrils, and we concluded that with these, K_3 is much larger (≥ 10) than with S1 (2−3). We can now explain this difference not by a difference in the cleavage step itself, but by different numbers of ADP·P_i states in the two systems. It is generally thought that the cleavage step occurs in the detached state, so we define K_3 as being equal to [M·ADP·P_i]/[M·ATP] whether in S1 or myofibrils (*7*, *56*, *57*). With S1 and if the the Bagshaw−Trentham scheme is assumed (Scheme 1), the P_i burst is due to one state only (M**·ADP·P_i). The concentrations of the M*·ADP·P_i state and free P_i are low because step 4 is slow and rate-limiting and step 5 is rapid and virtually irreversible.

However, with myofibrils, there is more than one ADP·P_i state before the rate-limiting P_i release, so K_3 cannot be obtained directly. Thus, in Scheme 4 (detached pathway) there are two and in Scheme 5 three such ADP·P_i states. Therefore, these accumulate in the steady state and are measured in the total P_i burst experiments. From the identity of the burst sizes in cold ATP chase and P_i burst experiments, it appears that in the steady state, with Scheme 4 [M·ADP·P_i] + [A∼M·ADP·P_i] ≈ [active site] and Scheme 5 [M·ADP·P_i] + [A∼M·ADP·P_i] + [A-M·ADP·P_i] ≈ [active site].

Steady State Parameters of Cross-Linked Myofibrils. The k_{cat} of XMF90 is less than 50% of that of un-cross-linked myofibrils, and in XMF120, k_{cat} is reduced further (Table 1). This reduction in k_{cat}, which is not due to a reduction in the ATPase site concentrations by the cross-linking procedure (see above), may be a reflection of the Fenn effect (*58*−*60*), namely, that the total energy liberated during a contraction is increased if the muscle is allowed to shorten, although with the two-pathway scheme this interpretation may be less clear-cut. With Scheme 5, it could be that the condition of the myofibril modulates the equilibria of the different (A)M·ADP·P_i states and that this, in turn, modulates the overall ATPase activity.

The rather sharp increase in the K_m for ATP upon cross-linking is noteworthy, especially the increase in going from 6.5 to 8% heads cross-linked (Table 1). This is surprising because cross-linked myofibrils appear to bind ATP as tightly as un-cross-linked myofibrils (with XMF120 in Figure 4). Further, consider the relation between k_2/K_1 and k_{cat}/K_m. With S1, these ratios are very similar [as expected if $k_{-2} \ll k_{cat}$ (*24*)]. With myofibrils, cross-linked or not, $k_2/K_1 > k_{cat}/K_m$. Unlike with S1, with myofibrils it is difficult to interpret k_{cat} and K_m in terms of individual rate constants. We have already referred to this problem elsewhere (*57*).

ACKNOWLEDGMENT

We are grateful to Michael Ferenczi, Corrado Poggesi, Robert Stehle, and Chiara Tesi for valuable discussions and Pierre Travo for help with the microscopy measurements.

REFERENCES

1. Bagshaw, C. R., and Trentham, D. R. (1974) *Biochem. J. 141*, 331−349.
2. Goldman, Y. E. (1987) *Annu. Rev. Physiol. 49*, 637−654.
3. Cooke, R. (1997) *Physiol. Rev. 77*, 671−697.
4. Siemankowski, R. F., Wiseman, M. O., and White, H. D. (1985) *Proc. Natl. Acad. Sci. U.S.A. 82*, 658−662.
5. Weiss, S., Rossi, R., Pellegrino, M. A., Bottinelli, R., and Geeves, M. A. (2001) *J. Biol. Chem. 276*, 45902−45908.
6. White, H. D., Belknap, B., and Webb, M. R. (1997) *Biochemistry 36*, 11828−11836.
7. Geeves, M. A., and Holmes, K. C. (1999) *Annu. Rev. Biochem. 68*, 687−728.
8. Dantzig, J. A., Goldman, Y. E., Millar, N. C., Lacktis, J., and Homsher, E. (1992) *J. Physiol. 451*, 247−278.
9. Morris, C., and Homsher, E. (1998) in *Current methods in muscle physiology*: *advantages, problems and limitations*, pp 71−89, Oxford University Press, Oxford, U.K.
10. Potma, E. J., van Graas, I. A., and Stienen, G. J. (1995) *Biophys. J. 69*, 2580−2589.
11. Brune, M., Hunter, J. L., Corrie, J. E., and Webb, M. R. (1994) *Biochemistry 33*, 8262−8271.
12. Ferenczi, M. A., and He, Z. H. (2002) *J. Muscle Res. Cell Motil.* (in press).
13. Bartoo, M. L., Popov, V. I., Fearn, L. A., and Pollack, G. H. (1993) *J. Muscle Res. Cell Motil. 14*, 498−510.
14. Friedman, A. L., and Goldman, Y. E. (1996) *Biophys. J. 71*, 2774−2785.
15. Colomo, F., Piroddi, N., Poggesi, C., de Kronnie, G., and Tesi, C. (1997) *J. Physiol. 500*, 535−548.
16. White, H. D. (1985) *J. Biol. Chem. 260*, 982−986.
17. Ma, Y. Z., and Taylor, E. W. (1994) *Biophys. J. 66*, 1542−1553.
18. Herrmann, C., Lionne, C., Travers, F., and Barman, T. (1994) *Biochemistry 33*, 4148−4154.
19. Herrmann, C., Houadjeto, M., Travers, F., and Barman, T. (1992) *Biochemistry 31*, 8036−8042.
20. Sleep, J. A. (1981) *Biochemistry 20*, 5043−5051.
21. Lionne, C., Brune, M., Webb, M. R., Travers, F., and Barman, T. (1995) *FEBS Lett. 364*, 59−62.
22. Barman, T., Brune, M., Lionne, C., Piroddi, N., Poggesi, C., Stehle, R., Tesi, C., Travers, F., and Webb, M. R. (1998) *Biophys. J. 74*, 3120−3130.
23. Herrmann, C., Sleep, J., Chaussepied, P., Travers, F., and Barman, T. (1993) *Biochemistry 32*, 7255−7263.
24. Biosca, J. A., Travers, F., Hillaire, D., and Barman, T. E. (1984) *Biochemistry 23*, 1947−1955.
25. Houadjeto, M., Travers, F., and Barman, T. (1992) *Biochemistry 31*, 1564−1569.
26. Barman, T. E., and Travers, F. (1985) *Methods Biochem. Anal. 31*, 1−59.
27. Reimann, E. M., and Umfleet, R. A. (1978) *Biochim. Biophys. Acta 523*, 516−521.
28. Woledge, R. C., Curtin, N. A., and Homsher, E. (1985) *Energetic aspects of muscle contraction*, Vol. 41, Academic Press, London.
29. Colomo, F., Nencini, S., Piroddi, N., Poggesi, C., and Tesi, C. (1998) *Adv. Exp. Med. Biol. 453*, 373−381.
30. Brandt, P. W., Colomo, F., Piroddi, N., Poggesi, C., and Tesi, C. (1998) *Biophys. J. 74*, 1994−2004.
31. Houadjeto, M., Barman, T., and Travers, F. (1991) *FEBS Lett. 281*, 105−107.
32. Tesi, C., Colomo, F., Piroddi, N., and Poggesi, C. (2002) *J. Physiol. 541*, 187−199.
33. Glyn, H., and Sleep, J. (1985) *J. Physiol. 365*, 259−276.
34. Lionne, C., Stehle, R., Travers, F., and Barman, T. (1999) *Biochemistry 38*, 8512−8520.
35. Trentham, D. R., Eccleston, J. F., and Bagshaw, C. R. (1976) *Q. Rev. Biophys. 9*, 217−281.
36. Malik, M. N., and Martonosi, A. (1972) *Arch. Biochem. Biophys. 152*, 243−257.
37. Trentham, D. R. (1977) *Biochem. Soc. Trans. 5*, 5−22.
38. Tesi, C., Kitagishi, K., Travers, F., and Barman, T. (1991) *Biochemistry 30*, 4061−4067.
39. Lionne, C., Travers, F., and Barman, T. (1996) *Biophys. J. 70*, 887−895.
40. Pate, E., and Cooke, R. (1989) *Pfluegers Arch. 414*, 73−81.
41. Johnson, R. E., and Adams, P. H. (1984) *FEBS Lett. 174*, 11−14.
42. Biosca, J. A., Greene, L. E., and Eisenberg, E. (1988) *J. Biol. Chem. 263*, 14231−14235.
43. Biosca, J. A., Travers, F., Barman, T. E., Bertrand, R., Audemard, E., and Kassab, R. (1985) *Biochemistry 24*, 3814−3820.
44. Sleep, J., Herrmann, C., Barman, T., and Travers, F. (1994) *Biochemistry 33*, 6038−6042.
45. Sleep, J. A., and Hutton, R. L. (1980) *Biochemistry 19*, 1276−1283.

46. Brune, M., Hunter, J. L., Howell, S. A., Martin, S. R., Hazlett, T. L., Corrie, J. E., and Webb, M. R. (1998) *Biochemistry 37*, 10370−10380.
47. Harada, Y., Sakurada, K., Aoki, T., Thomas, D. D., and Yanagida, T. (1990) *J. Mol. Biol. 216*, 49−68.
48. Tesi, C., Colomo, F., Nencini, S., Piroddi, N., and Poggesi, C. (2000) *Biophys. J. 78*, 3081−3092.
49. Huxley, A. F. (2000) *J. Biomech. 33*, 1189−1195.
50. Amitani, I., Sakamoto, T., and Ando, T. (2001) *Biophys. J. 80*, 379−397.
51. He, Z., Stienen, G. J., Barends, J. P., and Ferenczi, M. A. (1998) *Biophys. J. 75*, 2389−2401.
52. He, Z. H., Bottinelli, R., Pellegrino, M. A., Ferenczi, M. A., and Reggiani, C. (2000) *Biophys. J. 79*, 945−961.
53. Ranatunga, K. W. (1999) *Proc. R. Soc. London, Ser. B 266*, 1381−1385.
54. Málnási-Csizmadia, A., Woolley, R. J., and Bagshaw, C. R. (2000) *Biochemistry 39*, 16135−16146.
55. Geeves, M. A., Goody, R. S., and Gutfreund, H. (1984) *J. Muscle Res. Cell Motil. 5*, 351−361.
56. Lymn, R. W., and Taylor, E. W. (1971) *Biochemistry 10*, 4617−4624.
57. Stehle, R., Lionne, C., Travers, F., and Barman, T. (2000) *Biochemistry 39*, 7508−7520.
58. Huxley, A. F. (1980) *Reflections on muscle*, Liverpool University Press, Liverpool, U.K.
59. Huxley, A. F. (1957) *Prog. Biophys. Biophys. Chem. 7*, 255−318.
60. Kushmerick, M. J., and Davies, R. E. (1969) *Proc. R. Soc. London, Ser. B 174*, 315−353.

BI0260278